

LETTERS

Size Control and Associated Photophysics of Erbium-Doped Silicon Nanowires

Zhaoyu Wang and Jeffery L. Coffey*

Department of Chemistry, Texas Christian University, Fort Worth, Texas 76129

Received: July 24, 2003; In Final Form: October 9, 2003

Routes to different-sized Si nanowires with erbium-rich shell structures have been developed. Tunable nanowire widths with average values of 50, 75, 90, and 160 nm can be controlled by the nature of the gold catalyst employed in the vapor–liquid–solid reaction used to obtain the Si core structure. Lattice imaging of selected nanowires permit structural characterization as a single-crystal Si core surrounded by a polycrystalline erbium-rich surface layer. Furthermore, it appears that in relatively small wires (<100 nm in diameter), negligible near-infrared photoluminescence is observed, suggesting that energy transfer quenching by Er^{3+} clustering or surface hydroxyl groups on a relatively smaller surface area are likely origins for deactivation of the 1540 nm emission.

Semiconductor nanowires (NWs),¹ and silicon in particular (Si NWs),² are attracting extensive attention as a consequence of unique fundamental electronic and structural behavior relevant to device platforms. In the continuing evolution of wire architectures, the incorporation of dopant or impurity centers into a given nanowire is a logical step. The rare earth ion erbium is of particular interest for incorporation into crystalline Si because its ($^4\text{I}_{13/2} \rightarrow ^4\text{I}_{15/2}$) luminescent transition at 1.54 μm lies at a transmission maximum for silica based waveguides;^{3,4} selected properties of Si nanocrystals interacting with Er^{3+} ions suggest its novel utility as a laser material.⁵ Erbium-rich silicon phases also demonstrate enhanced conductivity, particularly as Schottky contacts on crystalline Si.⁶ Our group has achieved progress in the synthesis, characterization, and optical studies of Er-doped Si nanocrystals with dimensions of 3–25 nm by pyrolysis routes⁷ whereas others have employed plasma CVD/implantation methods for this same purpose.⁸ Moving beyond zero-dimensional dots, it is also important to fabricate one-dimensional nanoscale wires composed of Er^{3+} ions for potential value as components for both electrical and optical applications involving Si NWs relevant to sensing,⁹ information processing,¹⁰ etc. The propagation of light through a continuous Si nanowire network possessing the proper refractive index gradient (as a

consequence of erbium preferentially enriched at the wire surface) is an appealing concept in particular.

Previous work from our laboratories established the viability of a two-step pyrolysis process for the fabrication of erbium surface-enriched Si nanowires, where initially undoped Si nanowires are synthesized by a vapor–liquid–solid (VLS) method¹¹ followed by exposure of the as-made Si nanowires to the precursor $\text{Er}(\text{tmhd})_3$ at high temperature.¹² Wires of ~ 160 nm diameter were prepared from thermally evaporated Au films acting as catalytic sites for nucleation and growth of the silicon. It is important, however, to prepare such layered structures with different Si core widths to probe its size dependence on the optical properties of the rare earth center, specifically in this case the near-IR photoluminescence of Er^{3+} . In this study we achieve this comparison of doped Si NWs through the use of colloidal gold nanoparticles and sputtered gold films to direct the wire width in the VLS process; these results are compared with earlier data obtained for nanowire structures derived from thermally evaporated gold islands.

Experimental Section

Nanowire Synthesis. All silicon wafer samples were washed with water/ethanol and then heated at 70 °C for about 30 min in a 7:3 volume ratio of 98% H_2SO_4 :30% H_2O_2 , followed by a

* To whom correspondence should be addressed. E-mail: j.coffey@tcu.edu.

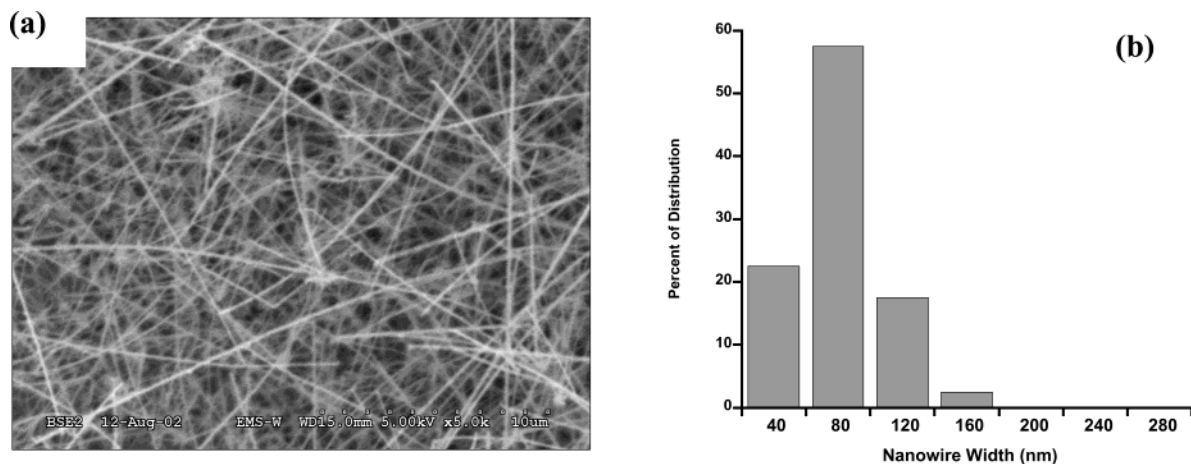


Figure 1. (a) SEM image of Er doped Si nanowires prepared using a colloidal Au catalyst. Dot to dot separation in the scale bar is 1 μm . (b) Histogram representing the size distribution of Er-doped Si NWs in this type of film.

final rinse with DI water immediately prior to use. In a typical experiment, a 5×15 mm piece of CZ Si containing a given type of Au catalyst is placed in an alumina boat, which is then positioned inside a quartz reactor. After annealing in He at ~ 600 $^{\circ}\text{C}$ for 1.5 h, SiH_4 is then introduced into the system at a flow rate of 40 sccm. This reactant is further diluted in He (at a flow rate of 3000 sccm), and the sample substrate is heated at a temperature of 600 $^{\circ}\text{C}$ for 2 min. In a subsequent step, erbium incorporation is achieved by passing He (at a flow rate of 3000 sccm) through the bubbler (heated to ~ 144 $^{\circ}\text{C}$) containing the $\text{Er}(\text{tmhd})_3$ precursor, which is consequently introduced into the pyrolysis oven. The oven temperature is maintained at about 600 $^{\circ}\text{C}$ for 30 min during Er incorporation. In a separate step, the resultant product is annealed in a vacuum at 900 $^{\circ}\text{C}$ for 1 h. Si NW samples were characterized with a combination of scanning electron microscopy (conventional SEM & field emission), transmission electron microscopy (TEM), high-resolution transmission electron microscopy (HREM), energy-dispersive X-ray spectroscopy (EDX), selected area electron diffraction (SAED), and Raman and photoluminescence (PL) spectroscopies.

Previous work by Lieber and co-workers has established the ability to control Si NW width through the use of diluted Au colloids of varying diameters adsorbed onto a Si surface in a VLS reaction.¹³ For our studies, we find that a combination of different catalyst preparation methods work best in this regard. One involves the use of gold colloids of 3.4 nm average diameter, prepared according to a literature procedure¹⁴ involving the reduction of AuCl_3 with NaBH_4 . A clean Si wafer was soaked in the as-formed Au colloid aqueous solution for a brief period of ~ 10 s. It was then removed quickly, dried in a gentle N_2 flow, and placed into the reactor. Additional Au catalyst samples were prepared on clean Si substrates using a RF sputter coater (Hummer VII) for either 5 or 25 s duration.

Instrumentation. Nanowire samples were characterized either using a JEOL JSM 6100 SEM at TCU or by the Electron Microscopy Facility at the University of Illinois at Chicago. For the latter, a Hitachi S-3000N VP-SEM was used to obtain the SEM images. TEM and EDX investigations were performed with a JEOL JEM-3010 with a ThermoNoran Vista EDX system. Near-IR photoluminescence (PL) spectra were obtained using an Applied Detector Corp. liquid- N_2 -cooled Ge-detector in conjunction with a Stanford Research Systems chopper/lock-in amplifier and an Acton Research Corp. 0.25 m monochromator. Sample excitation was provided by a Coherent Ar^+ laser, with collection optics identical to a setup previously described.⁷

Results and Discussion

Er-Doped Si NWs Prepared from Gold Colloids. In our initial studies on relatively large Si nanowires (prepared from thermally evaporated Au islands) and coated with an Er-rich phase at the surface, one could clearly visualize the presence of the erbium due to its enhanced contrast.¹² However, lattice imaging was not possible in these structures, so we consequently turned to a colloidal Au catalyst system to produce thinner wires and thus provide desired structural information about the Si/ ErSi_x interface. Typical results from the use of Au nanocrystals of 3.4 nm average diameter in the two-step reaction process are illustrated in Figure 1. This image shows a typical morphology for this type of Er-doped Si nanowire, with strongly interwoven structures that are microns long and noticeably rough on the surface. Wires produced by this process are typically ~ 10 – 15 μm in length. Conventional TEM imaging was used to generate size distributions of doped wire widths for this type of sample. A histogram to describe this distribution is illustrated in Figure 1b. It is evident that the annealing conditions for the gold catalyst are clearly sufficient for clustering of the individual nanocrystals, as the resultant Er-doped Si nanowires in this case have diameters between 20 and 145 nm, with an average of 75 nm.

Similar to Er-surface enriched Si nanowires prepared from a thermally evaporated Au film catalyst, higher magnification TEM analysis reveals the presence of dark contrast rims and light contrast cores. Corresponding EDX data for these regions indicate the presence of a higher Er concentration in the dark contrast surface (59 at. %) and a rather low Er doping level in the light contrast Si core (2.8 at. %). From the TEM image shown (Figure 2a) it is estimated that the Er-rich surface layer is about 5–7 nm in thickness. Crystallographically, selected area electron diffraction patterns (SAED) (Figure 2b) measured from this type of wire show both polycrystalline fringes (the observed ring pattern), which is attributed to the Er-rich surface and a single-crystal pattern (the array pattern of dots), which is associated with the Si core. Attempts to match the diffraction spacings in the polycrystalline Er-rich phase to a specific known erbium silicide phase have not been successful.

Lattice images reaching atomic resolution from these wires were obtained using high-resolution TEM (HRTEM). A typical HRTEM image from the edge of wire showing polycrystalline Er-rich grains (left) and single-crystal Si (right) is shown in Figure 3. These images were obtained by tilting a single nanowire to the 112 zone axis. By calculation of the lattice

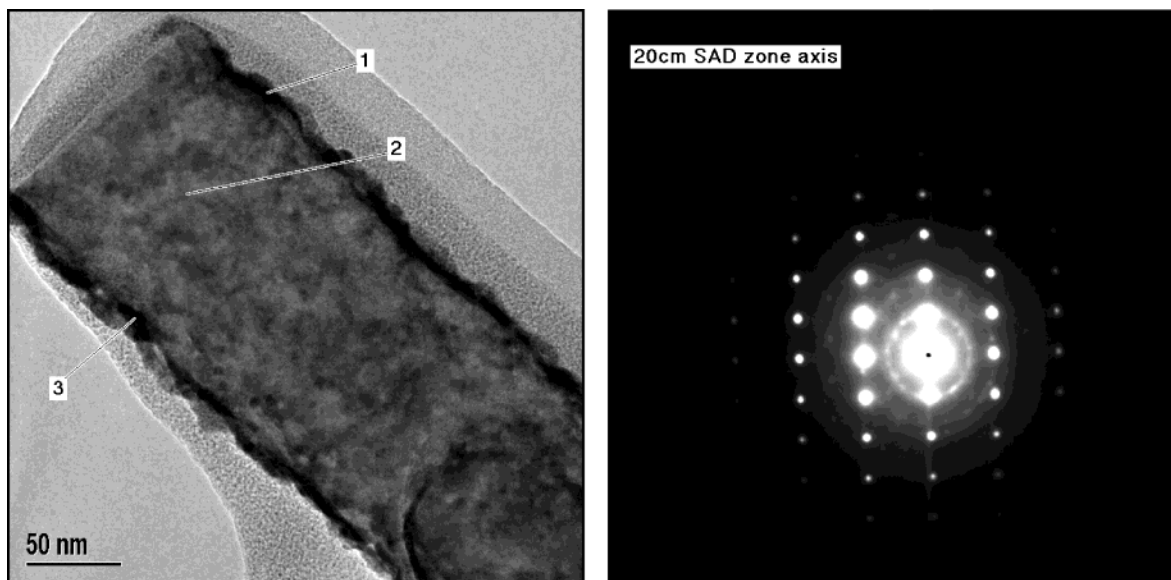


Figure 2. (a) TEM image of a single Er surface-enriched Si nanowire (~ 130 nm wide) prepared from the Au colloids. Scale bar is 50 nm. EDX analysis data reveals Er concentrations of 59.2, 2.8, and 58.8% and for the marked three areas marked 1, 2, and 3, respectively. (b) SAED pattern measured for a doped Si NW; both polycrystalline (surface) and single-crystal (core) features are observed.

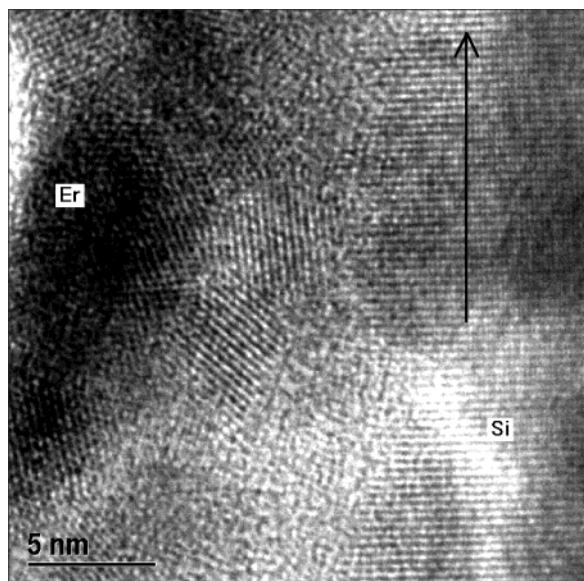


Figure 3. HREM image showing an Er-rich surface layer and Si core of a typical nanowire. Scale bar is 5 nm. The arrow shows the $\langle 111 \rangle$ lattice direction.

spacing, we can conclude that the single-crystal Si core grows along the $\langle 111 \rangle$ lattice direction because the spacing of the 111 plane (0.308 nm) is in good agreement with the observed value (0.32 nm).

Er-Doped Si NWs Prepared from Sputtered Gold Films.

Because of the ease of preparing relatively large catalyst surface areas in a single step, radio frequency-sputtered films also serve as active candidates in producing Si NWs of controlled size. In this regard, two types of gold films in terms of different sputtering duration were investigated: 5 and 25 s. Analysis of the morphologies of these films by field emission SEM (FE SEM) indicate that although both films reflect essentially continuous coverage, the 5 s sputtered sample produces gold features of tens of nanometers wide, whereas, as expected, the longer 25 s exposure generates gold structures of this regime, along with appreciably larger grains as well (> 100 nm, data not shown). Consequently, Er-doped Si nanowire samples produced from these samples reflect this difference in catalyst

dimension. A typical field emission SEM (FE SEM) image of an Er-doped Si nanowire sample prepared from a 5 s sputtered Au catalyst surface is presented in Figure 4a. Not surprisingly, SEM and FESEM images indicate that the Er-doped Si NWs prepared from 5 s sputtered gold film are much thinner and more uniform in distribution than those prepared from 25 s sputtered film. For the 5 s type of NWs, the diameters range from 20 to 100 nm with an average of ~ 50 nm, whereas for the 25 s type of NWs, the diameters range from 10 to 250 nm with an average of ~ 90 nm (Figure 4b). It is clear that the larger average size resulting from the longer sputter time (and catalyst dimension) comes at a cost of a significantly broader range of nanowire product sizes.

Photoluminescence Properties. Si NWs prepared from thermally evaporated Au catalysts (average Si NW width ~ 160 nm) and containing an Er-rich surface do exhibit the characteristic near-IR photoluminescence (PL) associated with the Er^{3+} centers if annealed briefly (900 $^{\circ}\text{C}$) after their preparation.¹² Having established viable routes to these layered structured nanowires of varying size, it is prudent to examine those conditions required to achieve this emission as a result of wire width.

Recalling that an anneal is necessary to detect the near-IR emission from such structures, we first decided to probe the origin of this activation in greater detail. The as-prepared 160 nm average diameter Er-doped Si nanowire samples have a brownish-black appearance compared to the brownish-yellow color of the undoped Si nanowires, which suggests the deposition of residual carbon onto the Si nanowire sample during the decomposition of $\text{Er}(\text{tmhd})_3$. After a low-vacuum anneal at 900 $^{\circ}\text{C}$, Raman spectra (not shown) show the disappearance (presumably as CO_2) of an amorphous carbon peak at ~ 1300 cm^{-1} , a feature not present in the original nanowire sample and not detected until Er^{3+} exposure. This anneal also serves the important purpose of activating the Er^{3+} ions, reducing Er^{3+} – Er^{3+} aggregation along the surface of the wire and providing noncentrosymmetric, parity-allowed transitions at the rare earth center through oxygen insertion reactions and local symmetry reduction.⁴ Erbium-rich Si phases, in the absence of oxygen, typically involve twelve-coordinate Er environments surrounded by Si that are nonluminescent.¹⁵

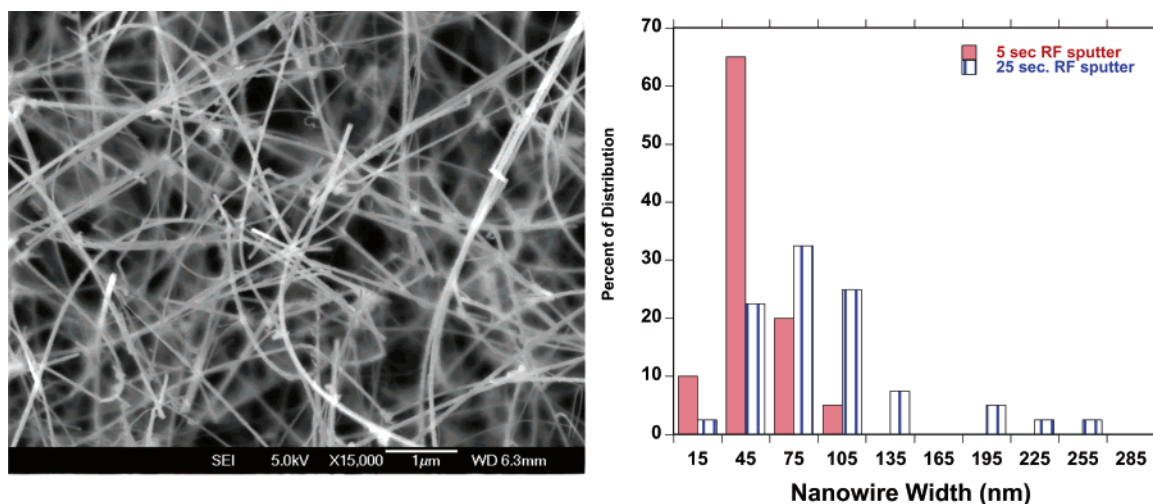


Figure 4. (a) Representative FE SEM image of Er-doped Si NWs prepared using a sputtered gold film of 5 s duration. (b) Histogram comparing distributions of nanowire width for Er-doped Si samples produced using 5 s Au catalyst sputter duration to those produced using a 25 s deposition period.

The photoluminescence spectra of the Er-doped Si nanowires prepared from the colloidal and RF sputtered Au catalysts was also measured using a procedure similar to that described above. Interestingly, the light emission efficiency for all three types of doped nanowire samples, with average diameters <100 nm, is so poor that it is effectively below the detection limit of our system. As a consequence, we can speculate that there are two factors contributing to this lack of PL intensity at 1540 nm. First, a clustering of the Er^{3+} centers on a relatively small surface area can play a role, as it is well-known from the literature that such clustering of Er^{3+} ions leads to a facile self-quenching process of the desired fluorescence by energy transfer between rare earth centers.¹⁶ Using known structural data (TEM results and bulk densities of cubic Si and ErSi_2), estimates of Er^{3+} concentrations for nanowires of both 160 and 70 nm diameter reveal a 3-fold greater concentration of erbium overall in the larger wires ($\sim 17\%$ versus 6%);¹⁷ however, there is something of a tradeoff here, as the exposed surface area in the 70 nm wide structure is smaller by a factor of 2.3. Hence there is the possibility of some concentration-induced self-quenching in such structures. In these smaller wires, a high-temperature anneal (at 900 °C) is apparently insufficient to locally alter enough Er^{3+} centers to induce optical activity. The second factor to take into consideration involves the possibility of OH-induced quenching in the smaller wires as a contributor to the diminished emission in the near-IR. Although all samples were exposed to identical thermal histories prior to emission measurements, it is reasonable to presume that a higher total Er concentration at the surface would result in a greater sensitivity to hydroxyl-induced quenching.

In summary, we have found facile routes for the formation of single-crystal Si nanowires coated with polycrystalline Er-rich Si surfaces, with the precise width strongly dictated by selection of catalyst and associated conditions. Photoluminescence data suggest a pragmatic limit as to erbium surface concentration for the wires synthesized to date; alternative strategies involving yet thinner erbium shells with lower resultant concentrations are in development, along with their subsequent photophysical and structural evaluation.

Acknowledgment. We thank the National Science Foundation and the Robert A. Welch Foundation for financial support

of this research. The expertise of Dr. Alan Nichols of the Electron Microscopy Facility of the Research Resources Center of the University of Illinois-Chicago is also gratefully acknowledged, along with useful assistance from Dr. Priyabrata Mukherjee in the synthesis of the gold nanocrystals.

References and Notes

- (1) Xia, Y.; Yang, P.; Sun, Y.; Wu, Y.; Mayers, B.; Gates, B.; Yin, Y.; Kim, F.; Yan, H. *Adv. Mater.* **2003**, *15*, 353.
- (2) Hu, J.; Odom, T. W.; Lieber, C. M. *Acc. Chem. Res.* **1999**, *32*, 435.
- (3) Polman, A. *J. Appl. Phys.* **1997**, *82*, 1.
- (4) Michel, J.; Assali, L. V. C.; Morse, M. T.; and Kimerling, L. C. *Semicond. Semimet.* **1998**, *49*, 111.
- (5) Kik, P. and Polman, A. In *Proceedings of the NATO Advanced Research Workshop "Optical Amplification and Stimulation in Silicon"*; Pavesi, L., Gaponenko, S., Dal Negro, L., Eds.; NATO Science Series II, Vol. 93; Kluwer: Dordrecht, The Netherlands, 2003; pp 383–400.
- (6) Norde, N.; de SousaPires, J.; d'Heurle, F.; Pessavento, F.; Peterson, S.; Tove, P. A. *Appl. Phys. Lett.* **1981**, *38*, 865.
- (7) St. John, J.; Coffey, J.; Chen, Y.; Pinizzotto, R. *J. Am. Chem. Soc.* **1999**, *121*, 1888. St. John, J.; Coffey, J.; Chen, Y.; Pinizzotto, R. *Appl. Phys. Lett.* **2000**, *77*, 1635. Senter, R.; Chen, Y.; Coffey, J.; Tessler, L. *Nanolett.* **2001**, *1*, 383. St. John, J.; Coffey, J. *J. Phys. Chem.* **2001**, *105*, 7599. Ji, J.; Senter, R.; Coffey, J. *Chem. Mater.* **2001**, *13*, 4783. Ji, J.; Coffey, J. *J. Phys. Chem.* **2002**, *106*, 3860. Tessler, L.; Coffey, J.; Ji, J.; Senter, R. *J. Non-Cryst. Solids* **2002**, 299–302P1, 673.
- (8) Kenyon, A. J.; Trwoga, P. F.; Federighi, M.; Pitt, C. W. *J. Phys. Cond. Matter* **1994**, *6*, L319. Fujii, M.; Yoshida, M.; Kanzawa, Y.; Hayashi, S.; Yamamoto, K. *Appl. Phys. Lett.* **1997**, *71*, 1198. Franzò, G.; Vinciguerra, V.; Priolo, F. *Appl. Phys. A* **1999**, *69*, 3. Kik, P. G.; Brongersma, M. L.; Polman, A. *Appl. Phys. Lett.* **2000**, *76*, 2325. Han, H. S.; Seo, S. Y.; Shin, J. H. *Appl. Phys. Lett.* **2001**, *79*, 4568. Franzò, G.; Boninelli, S.; Pacifici, D.; Priolo, F.; Iacona, F.; Bongiorno, C. *Appl. Phys. Lett.* **2003**, *82*, 3871.
- (9) Cui, Y.; Wei, Q.; Park, H.; Lieber, C. M. *Science* **2001**, *293*, 1289.
- (10) Cui, Y. and Lieber, C. M. *Science* **2001**, *291*, 851.
- (11) Wagner, R. S.; Ellis, W. C. *Appl. Phys. Lett.* **1964**, *4*, 89.
- (12) Wang, Z.; Coffey, J. L. *Nanolett.* **2002**, *2*, 1303.
- (13) Cui, Y.; Lauhon, L. J.; Gudiksen, M. S.; Wang, J.; Lieber, C. M. *Appl. Phys. Lett.* **2001**, *78*, 2214.
- (14) Patil, V.; Malvankar, R. B.; Sastry, M. *Langmuir* **1999**, *15*, 8197.
- (15) Adler, D. L.; Jacobson, D. C.; Eaglesham, D. J.; Marcus, M. A.; Benton, J. L.; Poate, J. M.; Citrin, P. H. *Appl. Phys. Lett.* **1992**, *61*, 2181.
- (16) Snoeks, E.; Kik, P.; Polman, A. *Opt. Mater.* **1996**, *5*, 159.
- (17) These estimates are based on wires of Si cores of 70 and 160 nm, respectively, with a 5 nm erbium disilicide layer for the smaller wires and a 20 nm erbium disilicide layer for the larger ones (from TEM analyses). Calculations were based on wires of 1 μm length. Concentrations are reported with respect to weight percent, using the densities of the cubic phase of Si and that of ErSi_2 .